Metaheuristic-Based Power Loss Optimization for Boost Converter Design

Le Anh Duc
School of Information and Communications Technology, Hanoi University of Industry, Hanoi, Vietnam
ducla@haui.edu.vn

Huy-Hoang Nguyen
School of Electrical and Electronic Engineering, Hanoi University of Industry, Hanoi, Vietnam
huyhoangbc14@gmail.com

Xuan Thanh Pham
School of Electrical and Electronic Engineering, Hanoi University of Industry, Hanoi, Vietnam
thanhpx@haui.edu.vn (corresponding author)

Received: 5 March 2026 | Revised: 18 March 2026 | Accepted: 29 March 2026

 DOI: https://doi.org/10.48084/etasr.18539

ABSTRACT

This article presents a design for a DC-DC Boost Converter (BoC), which is widely used in many power electronic systems. The objective of the optimization problem is to minimize power loss in circuit components to enhance the efficiency of the BoC while considering three variables: inductance, capacitance, and switching frequency. Leveraging nature-inspired metaheuristics, including a Bat Algorithm (BA) and a Differential Evolution (DE), enables the attainment of optimal solutions to the nonconvex problem. In numerous scenarios, the two proposed approaches outperform the two benchmarks: Geometric Programming (GP) and Particle Swarm Optimization (PSO). Additionally, the optimized BoCs successfully operate in PSIM, a circuit simulation software, thereby further validating the effectiveness of the design.

Keywords-bat algorithm; DC-DC boost converters; differential evolution; nature-inspired metaheuristics

I. INTRODUCTION

DC-DC converters play an important role in providing suitable voltage levels for power electronic systems, such as portable electronic devices [1-3], battery-operated equipment [4-6], and renewable energy applications [7-10]. In these systems, the supply voltage frequently fails to meet the required voltage levels. It is thus necessary to increase the voltage, especially in renewable energy sources that exhibit relatively low output voltages [7]. The Boost Converter (BoC) is frequently used to achieve voltage step-up due to its ease of use and reliable performance. Nonetheless, the power losses that occur during the energy conversion process are inevitable. The efficiency of DC-DC converters, including BoCs, is diminished and fails to reach the desired level, directly impacting the overall efficiency of the system [11, 12]. To enhance the overall performance of power electronic systems, it is essential to employ optimization methods to reduce losses and improve BoC efficiency.

Several studies have focused on optimizing DC-DC converters by directly modifying the duty cycle of power switches [13] or indirectly adjusting it using Proportional-Integral-Derivative (PID) and PI controllers [14-18]. The aforementioned studies have successfully enhanced control quality, but the methods employed predominantly optimized the control variables based on previously established hardware parameters. Specifically, the component specifications and the switching frequency were held constant throughout the optimization process. Consequently, the effects of design limitations, operational conditions, and loss distribution were not incorporated into the optimization problem.

This disadvantage has prompted the present work to seek a more effective method for mitigating power loss and enhancing the efficiency of the BoC. Authors in [19] analyzed the sensitivity of component specifications to DC-DC converter efficiency. Two studies concentrated on modifying component specifications for the BoC. Authors in [21] introduced an optimization approach employing Geometric Programming (GP) that applies to various DC-DC converters. The problem concerned minimizing power loss under various constraints, including Continuous Conduction Mode (CCM), and limits on inductor current and output-voltage ripple. From this foundation, authors in [22] further expanded their research by analyzing the sensitivity of BoC. This study revealed that the efficiency of the BoC is highly sensitive to inductance, capacitance, and switching frequency. At the same time, ripple

constraints and CCM significantly influence the BoC's ability to reduce power loss.

The effectiveness of Nature-Inspired Metaheuristics (NIMs) in DC-DC optimization methods has been highlighted. In [13, 18], a Particle Swarm Optimization (PSO) algorithm was employed, whereas in [14, 15], a flower pollination algorithm and whale optimization algorithm were utilized, respectively. Authors in [16] evaluated the efficacy of a grey wolf optimizer through a comparative analysis with a genetic algorithm and PSO.

The contributions of this study are: Initially, it further explores the application of NIMs in the design of DC-DC converters, proposing a Bat Algorithm (BA) and a Differential Evolution (DE) approach to optimize power loss in a BoC. Secondly, it examines the sensitivity of component specifications, including inductance, capacitance, and switching frequency, to BoC efficiency by treating them as optimization variables. Thirdly, the proposal is evaluated against two benchmarks: the GP approach in [20, 21] and the state-of-the-art PSO approach in numerous scenarios. Finally, the current work reassesses the optimized BoCs over the PSIM software specialized for circuit simulation.

II. MATHEMATICAL MODEL

A. Operating Principle

Figure 1 illustrates a fundamental BoC topology, in which L, C, and R represent the inductance, capacitance, and load resistance, respectively. D and Q indicate the diode and power switch, respectively, while Vin and Vout denote the input and output voltages. The operation of the BoC comprises two alternating states: 1) when Q is closed (Figure 1(b)), the circuit is in the charging phase for the inductor by V_{in}, and 2) when Q is opened (Figure. 1(c)), the inductor discharges the energy stored during 1) to the capacitor and the output load.

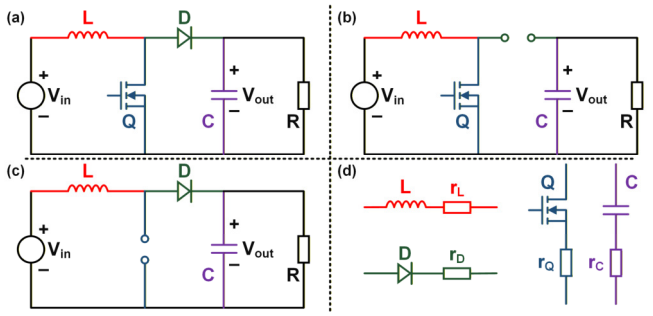

Fig. 1. A BoC topology. (a) Circuit. Equivalent circuit when (b) Q is closed and (c) Q is opened. (d) The parasitic resistance of components.

V_{out} is calculated as:

$$V_{out} = \frac{V_{in}}{1-\rho} \quad (1)$$

where $0 \leq \rho \leq 1$ is the duty cycle. The output voltage variation in 1) can be represented as:

$$\Delta v_{out,ON} = \frac{V_{out}\rho}{RCf_s} \quad (2)$$

where f_s is the switching frequency. In the CCM, both the inductor current and output voltage ripples have a triangular form, and they can be calculated as:

$$\Delta i_L = \Delta i_{L,ON} = \frac{V_{in}\rho}{Lf_s} \quad (3)$$

$$\Delta v_{out} = \Delta v_{out,ON} = \frac{V_{out}\rho}{RCf_s} \quad (4)$$

To ensure that the BoC is in CCM, L must satisfy the condition:

$$L > \frac{\rho(1-\rho)^2 R}{2f_s} \quad (5)$$

B. Power Loss Analysis

Figure 1(a) presents an ideal BoC model, in which neither passive nor semiconductor components exhibit loss. However, in practice, it is significant to account for the parasitic factor, which is the main cause of efficiency reduction. Figure 1(d) shows how the parasitic factor is displayed as resistance.

The dissipated power by the diode can be presented as:

$$P_D = V_{TH,D} I_{out} + \frac{r_D I_{out}^2}{1-\rho} \quad (6)$$

where r_D is the resistance when D is forward biased, and $V_{TH,D}$ is the D threshold voltage. The dissipated power by the inductor, P_L, is formulated as:

$$P_L = \left(\left(\frac{I_{out}}{1-\rho}\right)^2 + \frac{\Delta i_L^2}{12}\right) r_L \quad (7)$$

where r_L is the L parasitic resistance. The power consumption of the switch, which comprises conduction and switching losses, is given by:

$$\begin{aligned} P_Q = & \left(\left(\frac{I_{out}}{1-\rho}\right)^2 + \frac{\Delta i_L^2}{12}\right)\rho r_Q \\ & + \left(V_{out} - V_{TH,Q}\right)\left(\frac{I_{out}}{1-\rho} - \frac{\Delta i_L}{2}\right) T_{SW,ON} f_s \\ & + \left(V_{out} - V_{TH,Q}\right)\left(\frac{I_{out}}{1-\rho} + \frac{\Delta i_L}{2}\right) T_{SW,OFF} f_s \end{aligned} \quad (8)$$

where I_{out} is the output current, r_Q is the resistance when Q is closed, and $V_{TH,Q}$ is the Q threshold voltage. $T_{SW,ON}$ and $T_{SW,OFF}$ are, respectively, the switching times from the ON state to the OFF state and vice versa. The dissipated power by the capacitor is formulated as:

$$P_C = I_C^2 r_C \quad (9)$$

where r_C is the C parasitic resistance. In (9), IC is the Root Mean Square (RMS) C current, and is determined as:

$$\begin{aligned} I_C^2 = & \left(1-\rho^3\right)\frac{\left(I_{max}-I_{min}\right)^2}{3f_s\left(1-\rho\right)^2} + \left(\rho^2-1\right)\frac{\left(I_{max}-I_{min}\right)\left(I_{max}-I_{out}\right)}{f_s\left(1-\rho\right)} \\ & + \left(1-\rho\right)\frac{\left(I_{max}-I_{out}\right)^2}{f_s} + \frac{I_{out}^2\rho}{f_s} \end{aligned} \quad (10)$$

The total power loss of the BoC can be calculated as:

$$P_{loss} = P_Q + P_D + P_L + P_C \quad (11)$$

The efficiency of the BoC is then computed as:

$$\eta = \frac{P_{load}}{P_{load}+P_{loss}} 100\% \quad (12)$$

where $P_{load} = V_{out} I_{out}$ is the useful power.

III. PROPOSED METAHEURISTIC-BASED APPROACHES

A. Problem Formulation and Penalty Method

The optimization problem is formulated as:

$$\begin{aligned} \min_{L,C,f_s} \quad & P_{loss} \\ \text{s. t.} \quad & C1{:}\Delta i_L \le \gamma_i I_{out}, \\ & C2{:}\Delta v_{out} \le \gamma_v V_{out}, \\ & C3{:}\text{Eq. (5)} \end{aligned} \quad (13)$$

where I and V correspond to the acceptable current and voltage ripples. In (13), C1 and C2 control the inductor current and output-voltage ripples, respectively, while C3 maintains the BoC to ensure CCM operation. This problem can be reformulated as:

$$\begin{aligned} \min_{L,C,f_s} \quad & P_{loss} \\ \text{s. t.} \quad & C1{:}\Delta i_L - \gamma_i I_{out} \le 0, \\ & C2{:}\Delta v_{out} - \gamma_v V_{out} \le 0, \\ & C3{:}R\rho(1-\rho)^2 - 2Lf_s < 0 \end{aligned} \quad (14)$$

By using the penalty method, (14) can be expressed as:

$$\min_{L,C,f_s} O = [P_{loss} + K] \quad (15)$$

where K is the penalty term and can be written in detail as:

$$\begin{aligned} K = {} & \beta_1 \max\{0, \Delta i_L - \gamma_i I_{out}\}^2 + \beta_2 \max\{0, \Delta v_{out} - \gamma_v V_{out}\}^2 \\ & + \beta_3 \max\left\{0, R\rho(1-\rho)^2 - 2Lf_s\right\}^2 \end{aligned} \quad (16)$$

where $\{\beta_1, \beta_2, \beta_3\} > 0$ are the penalty factors.

B. Differential Evolution-Based Approach

DE is based on the mechanism involving three main operators: mutation, crossover, and selection [22, 23]. In mutation, with each individual $x_i = [L_i, C_i, f_{s,i}]$, $i \in \{1, \dots, N\}$, where N is the size of the population, three different vectors x_a, x_b, and x_c are randomly picked from the population to create a donor vector at the t-generation as:

$$v_i^{(t)} = x_a^{(t-1)} + F\left(x_b^{(t-1)} - x_c^{(t-1)}\right) \quad (17)$$

where F is a differential factor that decides the disturbance. The donor vector is then combined with the original individual via the probable crossover as:

$$u_{i,j}^{(t)} = \begin{cases} v_{i,j}^{(t)} & \text{rand} \le C_r \\ x_{i,j}^{(t-1)} & \text{otherwise} \end{cases}, j \in \{1,2,3\} \quad (18)$$

where $\text{rand}: U(0,1)$ and C_r is the crossover probability. Finally, the selection helps keep the better individual as:

$$x_i^{(t)} = \begin{cases} u_{i,j}^{(t)} & O\left(u_{i,j}^{(t)}\right) \le O\left(x_i^{(t-1)}\right) \\ x_i^{(t-1)} & i \in \{1, \dots, N\} \end{cases} \quad (19)$$

C. Bat Algorithm-Based Approach

BA is based on the following rules [24, 25]: First, each bat uses echolocation to recognize and distinguish the target from the barrier, and then to estimate the distance to the prey. Secondly, the bat moves in the search domain with the velocity v_i at the location/solution x_i and simultaneously emits the pulse with the loudness A and emission rate r. To simplify the implementation of BA, both A and r are fixed.

The frequency of the pulse can be written as:

$$f_i = f_{min} + (f_{max} - f_{min})\text{rand} \quad (20)$$

where f_{min} and f_{max} correspond to the minimum and maximum pulse frequency. The velocity and solution at the t-generation are expressed as:

$$v_i^{(t)} = v_i^{(t-1)} + \left(x_i^{(t-1)} - x_*\right) f_i \quad (21)$$

$$x_i^{(t)} = x_i^{(t-1)} + v_i^{(t)} \quad (22)$$

where x_* is the current best solution. If $\text{rand} > r$, bat creates a new local solution around x_*:

$$x_i = x_* + 0.01(x_{max} - x_{min})\text{rand} \quad (23)$$

However, only if $\text{rand} < A$, bat accepts this new solution.

IV. NUMERICAL RESULTS

A. Simulation Setup

In this study, the BoC parameters are adopted from previously published works [20, 21] across all simulations to ensure a fair comparison of approaches. In which V_{in} is fixed at 5 V, while V_{out} is investigated over the range 10 V to 45 V in 5 V steps. The on-state resistance of both Q and D is set to 5.2 mΩ. The turn-on and turn-off times of Q are both set to 10^{-8} s. The threshold voltages of Q and D are set to 0.9 V. The design parameters are constrained within predefined bounds. L ranges from $\{L_{min}, L_{max}\} = \{0.1, 10^4\}$ μH, while C and f_s are bounded with μF and $\{f_{s,min}, f_{s,max}\} = \{10{,}800\}$ kHz, respectively. In addition, $\gamma_i = 15\%$ and $\gamma_v = 1\%$.

In DE, F = 0.7 helps maintain a stable mutation disturbance, while $C_r = 0.9$ promotes high success from the donor vector. In BA, f_i is in the range of open $\{f_{min}, f_{max}\} = \{0,2\}$, and A and r are fixed at 0.5. The penalty factors gradually increase versus iteration as $\{\beta_1, \beta_2, \beta_3\} = 100t^2$. Finally, the optimization simulations are executed in MATLAB before being reassessed in PSIM.

B. Performance Comparison

Initially, the current study compares the two proposed approaches with the GP in [20, 21] and the PSO in two cases: V_{out} = 10 V and V_{out} = 45 V. This study sets N = 50 for all NIMs in the whole simulation.

Figure 2 illustrates the optimization results over 1000 iterations of approaches in the case of V_{out} = 10 V. As evidenced in Figure 2(a), P_{loss} of the GP approach is the greatest at 2.1 W, while all NIMs have a P_{loss} that is approximately 2 W. Between NIMs, the DE and BA approaches have the same performance. Meanwhile, the PSO approach has a P_{loss} higher than 1.96 W, indicating this lack of exploration when mainly relying on the previous walks of the best individual. Indeed, in Figure 2(b), while the DE and BA approaches converge to their respective L values, the PSO approach does not do so after the maximum number of iterations. Also, the GP approach reaches a minute value for this component. This phenomenon, along with f_s (Figure 2(c)) and C (Figure 2(d)), which only achieve values close to those of the DE and BA approaches, contributes to the higher power loss observed in the GP approach.

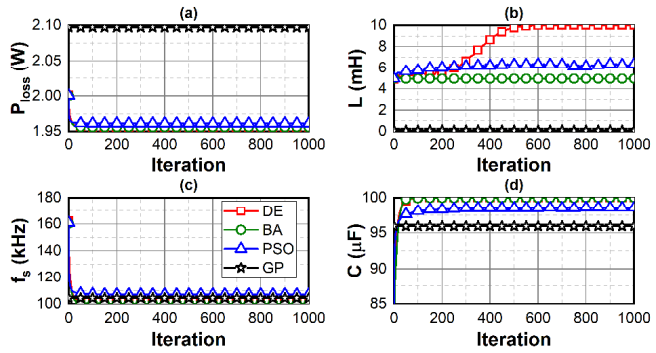

Fig. 2. (a) P_{loss}, (b) inductance, (c) switching frequency, and (d) capacitance over iterations of DE, BA, PSO, and GP approaches. Case 1: V_{out} = 10 V.

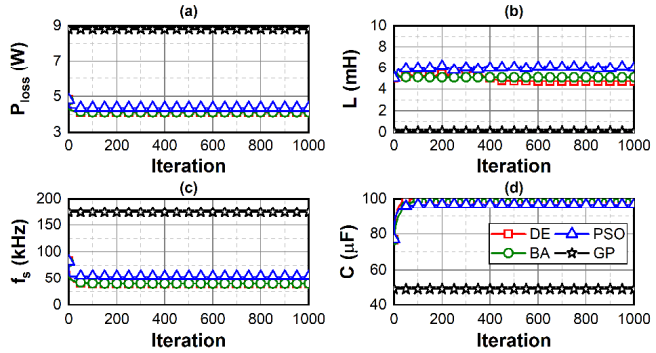

Fig. 3. (a) P_{loss}, (b) inductance, (c) switching frequency, and (d) capacitance over iterations of DE, BA, PSO, and GP approaches. Case 2: V_{out} = 45 V.

Figure 3 demonstrates the optimization results over 1000 iterations for the approaches at Vout = 45 V. Analogous to the case of Vout = 10 V (Figure 3(a)), Ploss is in ascending order, starting with the GP approach and progressing to the DE and BA approaches. Also, in Figure 3(b), the *L* of the GP approach is significantly smaller than the others, and that of the PSO approach oscillates instead of being stable. Regarding fs and C, as presented in Figures 3(c) and 3(d), there is a distinction between the GP and PSO approaches: the GP approach consistently shows the greatest distance, while the PSO approach is closer to the DE and BA approaches.

This work investigates the operation of the BoC over a range from 10 V to 45 V with four metrics: L, f_s, C, and the efficiency of the BoC. Figure 4(a) presents the inductance L as a function of V_{out} for three metaheuristic approaches. It can be observed that the DE approach decreases from the maximum value in the search domain, while the BA and PSO approaches oscillate around 5 mH and 6 mH, respectively. In contrast to L, f_s reduces from about 100 kHz to approximately 40 kHz, as illustrated in Figure 4(b). Compared to the others, the PSO approach consistently yields higher values, and this gap widens as V_{out} increases. This factor, along with the smaller and lower value of C (Figure 4(c)), is the main reason the efficiency of the PSO approach is worse than that of the DE and BA approaches, as shown in Figure 4(d). Moreover, the efficiency of all approaches increases proportionally with V_{out}. Authors in [20, 21] reported BoC efficiencies of 90.5% and 91.084% for V_{out} = 10 V and V_{out} = 45 V, respectively, which are much lower than those of NIMs, particularly the two proposed approaches.

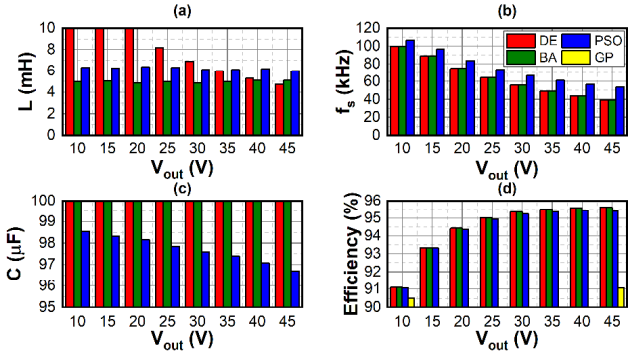

Fig. 4. (a) Inductance, (b) switching frequency, (c) capacitance, and (d) efficiency over V_{out} of DE, BA, and PSO approaches.

C. Circuit Simulation via PSIM

Figure 5 depicts a BoC in PSIM software, where, in addition to the basis of a BoC, three measurement points, namely I_L, I_{out}, and V_{out}, are set.

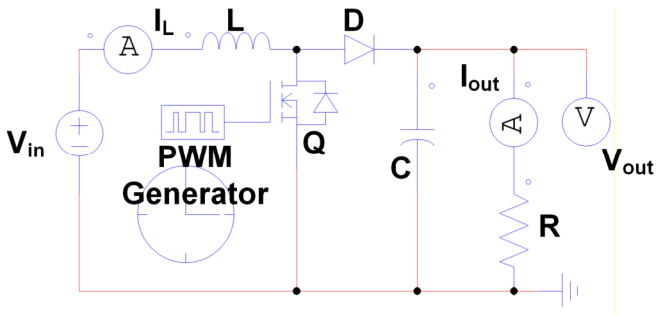

Fig. 5. A BoC in PSIM.

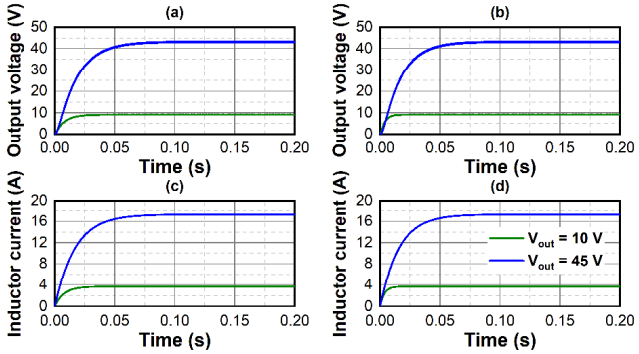

Fig. 6. Output voltage over time of: (a) the DE approach and (b) the BA approach. Inductor current over time of: (c) the DE approach and (d) the BA approach.

Figure 6(a) displays the output voltage waveform for two cases: V_{out} = 10 V and V_{out} = 45 V. The BoC responses exhibit a slight voltage drop across the components in both cases. Figure 6(b) plots the output voltage waveform using the BA solutions in those cases. Compared with the DE approach, the solution of the BA approach makes the BoC transient faster in the case of V_{out} = 10 V. Figures 6(c) and 6(d) present the input current waveform using the DE and BA solutions in two cases of V_{out} = 10 V and V_{out} = 45 V. It can be observed that the current curves have the same form as the voltage curves.

Finally, the efficiency of all approaches is measured, as illustrated in Figure 7. In contrast with the computational efficiency, as portrayed in Figure 4(c), the simulation efficiency in PSIM shows the approximation between the approaches. The dissimilarity between computation and simulation is clear: e.g., at V_{out} = 10 V, the simulation efficiency decreases by about 0.5% for NIMs, while the GP approach shows only an insignificant increase; from V_{out} = 20 V onward, the simulation efficiency is much higher than the computational efficiency. Although the efficiency in this work is reported as 91.084%, when simulated in PSIM, the efficiency documented in [21] increases to 96%, matching that of the PSO approach; however, both are lower than the two proposed approaches. The same thing occurs with the two proposed approaches when, at some points, the simulation efficiency of the BA approach is better than that of the DE approach.

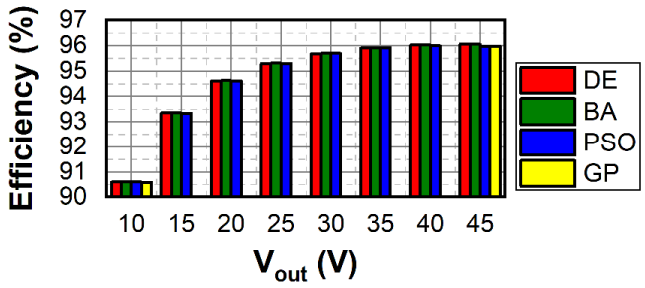

Fig. 7. Simulation efficiency over V_{out} of DE, BA, PSO, and GP approaches in PSIM.

V. CONCLUSION

This study provides a basis for optimizing DC-DC converters by implementing Nature-Inspired Metaheuristic (NIM)-based approaches. It also contributes to developing and analyzing mathematical frameworks for more complex DC-DC systems and for employing advanced optimization techniques. After acquiring extensive knowledge of this field, it becomes feasible to experiment with the actual system and apply it to real-world situations.

DECLARATION OF COMPETING INTERESTS

The author declares that there are no competing interests.

ACKNOWLEDGEMENT

This research is funded by Hanoi University of Industry under Contract No. 47-2025-RD/HD-DHCN.

DATA AVAILABILITY

The data supporting the findings of this study are available from the author upon reasonable request.

REFERENCES

[1] K. Bendaoud, J. Laassiri, S. Krit, and L. El Maimouni, "Design and simulation DC-DC power converters buck and boost for mobile applications using Matlab/Simulink," in *2016 International Conference on Engineering & MIS (ICEMIS)*, Sep. 2016, pp. 1–6, https://doi.org/10.1109/ICEMIS.2016.7745361.

[2] K. Zhang, "A Compact Digital-Controlled Soft-Start Circuit of DC-DC Switching Converter for Portable Devices," in *2022 IEEE 4th International Conference on Circuits and Systems (ICCS)*, Sep. 2022, pp. 86–90, https://doi.org/10.1109/ICCS56666.2022.9936264.

[3] J. Cao, B. Chen, H. Ye, and J. Feng, "A Boost DC-DC Converter with Low Power and High Efficiency for Portable Device Applications," in *2025 IEEE 16th International Conference on ASIC (ASICON)*, Jul. 2025, pp. 1–5, https://doi.org/10.1109/ASICON66040.2025.11326509.

[4] M. Elhebeary and C.-K. K. Yang, "A 92%-Efficiency Battery Powered Hybrid DC-DC Converter for IoT Applications," *IEEE Transactions on Circuits and Systems I: Regular Papers*, vol. 67, no. 10, pp. 3342–3351, July 2020, https://doi.org/10.1109/TCSI.2020.2979495.

[5] Y.-S. Noh, J.-I. Seo, H.-S. Kim, and S.-G. Lee, "A Reconfigurable DC-DC Converter for Maximum Thermoelectric Energy Harvesting in a Battery-Powered Duty-Cycling Wireless Sensor Node," *IEEE Journal of Solid-State Circuits*, vol. 57, no. 9, pp. 2719–2730, Sep. 2022, https://doi.org/10.1109/JSSC.2022.3152261.

[6] S. Palazzo *et al.*, "Multi-Objective Design of a Bidirectional DC-DC Converter for Battery-Powered Locomotive," in *2024 IEEE International Conference on Electrical Systems for Aircraft, Railway, Ship Propulsion and Road Vehicles & International Transportation Electrification Conference (ESARS-ITEC)*, Aug. 2024, pp. 1–7, https://doi.org/10.1109/ESARS-ITEC60450.2024.10819834.

[7] P. Poure, S. Weber, B. Vidales, M. Madrigal, and D. Torres, "High step-up DC-DC converter for renewable energy harvesting applications," in *2016 IEEE 16th International Conference on Environment and Electrical Engineering (EEEIC)*, Jun. 2016, pp. 1–6, https://doi.org/10.1109/EEEIC.2016.7555767.

[8] P. K. Maroti, S. Padmanaban, P. Wheeler, F. Blaabjerg, and M. Rivera, "Modified high voltage conversion inverting cuk DC-DC converter for renewable energy application," in *2017 IEEE Southern Power Electronics Conference (SPEC)*, Sep. 2017, pp. 1–5, https://doi.org/10.1109/SPEC.2017.8333675.

[9] S. Hasanpour, Y. P. Siwakoti, and F. Blaabjerg, "A New High Efficiency High Step-Up DC/DC Converter for Renewable Energy Applications," *IEEE Transactions on Industrial Electronics*, vol. 70, no. 2, pp. 1489–1500, Oct. 2023, https://doi.org/10.1109/TIE.2022.3161798.

[10] S. M. Hashemzadeh and B. Zhu, "Dual-Input Single-Output Voltage Multiplier-Based High Step-Up Converter for Renewable Energy Integration in DC Microgrids," *IEEE Transactions on Power Electronics*, vol. 41, no. 5, pp. 7884–7897, Feb. 2026, https://doi.org/10.1109/TPEL.2025.3635678.

[11] Z. Ivanovic, B. Blanusa, and M. Knezic, "Power loss model for efficiency improvement of boost converter," in *2011 XXIII International Symposium on Information, Communication and Automation Technologies*, Jul. 2011, pp. 1–6, https://doi.org/10.1109/ICAT.2011.6102129.

[12] G. Marsala, G. A. Farulla, M. Ferraro, and M. Luna, "A new Boost DC-DC Quadratic Converter: Power Loss and Conversion Efficiency Analysis," in *2025 IEEE 3rd International Power Electronics and Application Symposium (PEAS)*, Aug. 2025, pp. 1045–1049, https://doi.org/10.1109/PEAS66638.2025.11403512.

[13] J. Zhao *et al.*, "An Optimized Multi-Level Control Method for Wireless Power Transfer System Using the Particle Swarm Optimization Algorithm," *Electronics*, vol. 13, no. 22, Jan. 2024, Art. no. 4341, https://doi.org/10.3390/electronics13224341.

[14] T. Wiangtong and J. Sirapatcharangkul, "PID design optimization using flower pollination algorithm for a buck converter," in *2017 17th International Symposium on Communications and Information Technologies (ISCIT)*, Sep. 2017, pp. 1–4, https://doi.org/10.1109/ISCIT.2017.8261202.

[15] B. Hekimoğlu, S. Ekinci, and S. Kaya, "Optimal PID Controller Design of DC-DC Buck Converter using Whale Optimization Algorithm," in *2018 International Conference on Artificial Intelligence and Data Processing (IDAP)*, Sep. 2018, pp. 1–6, https://doi.org/10.1109/IDAP.2018.8620833.

[16] J. Águila-León, C. D. Chiñas-Palacios, C. Vargas-Salgado, E. Hurtado-Perez, and E. X. M. García, "Optimal PID Parameters Tunning for a DC-DC Boost Converter: A Performance Comparative Using Grey Wolf Optimizer, Particle Swarm Optimization and Genetic Algorithms," in *2020 IEEE Conference on Technologies for Sustainability (SusTech)*, Apr. 2020, pp. 1–6, https://doi.org/10.1109/SusTech47890.2020.9150507.

[17] A. Mamizadeh, N. Genc, and R. Rajabioun, "Optimal Tuning of PI Controller for Boost DC-DC Converters Based on Cuckoo Optimization Algorithm," in *2018 7th International Conference on Renewable Energy Research and Applications (ICRERA)*, Jul. 2018, pp. 677–680, https://doi.org/10.1109/ICRERA.2018.8566883.

[18] A. Debnath, T. O. Olowu, S. Roy, I. Parvez, and A. Sarwat, "Particle Swarm Optimization-based PID Controller Design for DC-DC Buck Converter," in *2021 North American Power Symposium (NAPS)*, Aug. 2021, pp. 1–6, https://doi.org/10.1109/NAPS52732.2021.9654737.

[19] N. Hinov, P. Stanchev, and G. Vacheva, "Analysis and Optimization of DC-DC Converters Through Sensitivity to Parametric Variations," *Technologies*, vol. 13, no. 2, Feb. 2025, Art. no. 56, https://doi.org/10.3390/technologies13020056.

[20] U. Ribes-Mallada, R. Leyva, and P. Garcés, "Optimization of DC-DC Converters via Geometric Programming," *Mathematical Problems in Engineering*, vol. 2011, no. 1, Sep. 2011, Art. no. 458083, https://doi.org/10.1155/2011/458083.

[21] U. Ribes-Mallada, R. Leyva, and P. Garcés, "Sensitivity analysis in boost converters optimal design," in *11th International Conference on Electrical Power Quality and Utilisation*, Jul. 2011, pp. 1–6, https://doi.org/10.1109/EPQU.2011.6128898.

[22] R. Storn, "On the usage of differential evolution for function optimization," in *Proceedings of North American Fuzzy Information Processing*, Jun. 1996, pp. 519–523, https://doi.org/10.1109/NAFIPS.1996.534789.

[23] R. Storn and K. Price, "Differential Evolution – A Simple and Efficient Heuristic for global Optimization over Continuous Spaces," *Journal of Global Optimization*, vol. 11, no. 4, pp. 341–359, Dec. 1997, https://doi.org/10.1023/A:1008202821328.

[24] X.-S. Yang, "A New Metaheuristic Bat-Inspired Algorithm," in *Nature Inspired Cooperative Strategies for Optimization (NICSO 2010)*, J. R. González, D. A. Pelta, C. Cruz, G. Terrazas, and N. Krasnogor, Eds. Berlin, Heidelberg: Springer, 2010, pp. 65–74.

[25] X. Yang and A. Hossein Gandomi, "Bat algorithm: a novel approach for global engineering optimization," *Engineering Computations*, vol. 29, no. 5, pp. 464–483, Jul. 2012, https://doi.org/10.1108/02644401211235834.